Effect of discontinuity in the threshold distribution on the critical behavior of a random fiber bundle

Uma Divakaran* and Amit Dutta†
Department of Physics, Indian Institute of Technology, Kanpur-208016, India
(Received 21 August 2006; revised manuscript received 16 October 2006; published 19 January 2007)

The critical behavior of a random fiber bundle model with mixed uniform distribution of threshold strengths and global load sharing rule is studied with a special emphasis on the nature of distribution of avalanches for different parameters of the distribution. The discontinuity in the threshold strength distribution of fibers nontrivially modifies the critical stress as well as puts a restriction on the allowed values of parameters for which the recursive dynamics approach holds good. The discontinuity leads to a nonuniversal behavior in the avalanche size distribution for smaller values of avalanche size. We observe that apart from the mean field behavior for larger avalanches, a new behavior for smaller avalanche size is observed as a critical threshold distribution is approached. The phenomenological understanding of the above result is provided using the exact analytical result for the avalanche size distribution. Most interestingly, the prominence of nonuniversal behavior in avalanche size distribution depends on the system parameters.

DOI: 10.1103/PhysRevE.75.011117 PACS number(s): 64.60.Ht, 81.05.Ni, 46.50.+a, 62.20.Mk

I. INTRODUCTION

Breakdown phenomena in nature has captured the attention of scientists for years [1]. A study of this phenomena plays a major role for the prediction of failure and design of materials and structures. One of the paradigmatic model mimicking the fracture processes is the random fiber bundle model (RFBM) which is simple yet subtle enough to capture the essential physics of the breakdown phenomena.

Random fiber bundle models [2–5] have been studied extensively in recent years. Typically a RFBM consists of N parallel fibers with randomly distributed threshold strength (σ_{th}) taken from a given distribution. If the stress generated due to an external force is greater than σ_{th} of a fiber, it breaks. The dynamics of the model is initiated by applying a small external force just enough to break the weakest fiber present in the bundle. The load carried by this broken fiber is shared amongst the remaining intact fibers following a load sharing rule causing further failures. When no further failure takes place, the external force is once again increased quasistatically to break the weakest intact element present in the bundle and the process continues until the bundle breaks down completely at an external stress called the critical stress. Even though the threshold distribution of real materials may not be known exactly, in theoretical models the distributions are usually approximated by either a uniform distribution or a Weibull distribution [3].

The avalanche size is defined as the number of broken fibers between two successive loadings. The distribution of avalanche size turns out to be a key factor in charaterizing any breakdown phenomena. Hemmer and Hansen [6] studied the avalanche size distribution $D(\Delta)$ of an avalanche of size Δ in a RFBM with the global load sharing (GLS) scheme, in which the additional stress due to a broken fiber is distributed equally to the remaining intact fibers. They established a universal power-law distribution in the large Δ limit given as $D(\Delta) \propto \Delta^{-\xi}$ with $\xi = 5/2$.

RFBM with threshold strengths which are continuous and are uniformly distributed between 0 to σ_1 and also between σ_2 to 1 [3,4], have been studied separately. But what happens when two such bundles are merged is not known, especially when $\sigma_1 < \sigma_2$ such that there exists a discontinuity in the threshold strength distribution. In this paper, we investigate the role of such a discontinuity on the critical behavior of a RFBM. The distribution of threshold strength of fibers used in the present work is given as (see Fig. 1)

$$\rho(\sigma_{th}) = \frac{1}{1-(\sigma_2-\sigma_1)}, \quad 0 < \sigma_{th} \leq \sigma_1,$$

$$= 0, \quad \sigma_1 < \sigma_{th} < \sigma_2,$$

$$= \frac{1}{1-(\sigma_2-\sigma_1)}, \quad \sigma_2 \leq \sigma_{th} \leq 1. \tag{1}$$

The discontinuity as defined above introduces dilution in the model in the sense that two types of fibers separated by a gap in their threshold distributions coexist in the same bundle. It is shown below that this discontinuity plays a crucial role in the dynamics of the model. Here, a fraction f of fibers belong to the weaker threshold distribution with strengths uniformly lying between 0 and σ_1 (Class A) whereas the remaining

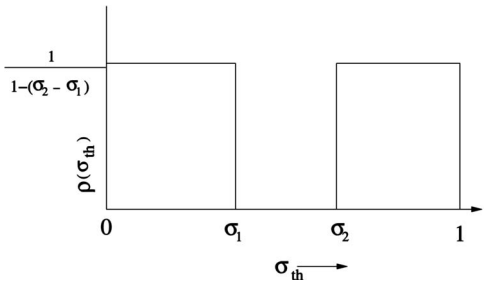

FIG. 1. Mixed uniform distribution

*Electronic address: udiva@iitk.ac.in
†Electronic address: dutta@iitk.ac.in

fraction of fibers have stronger threshold strengths between σ_2 and 1 (Class B). Clearly, $(\sigma_2-\sigma_1)$ is the measure of the discontinuity which vanishes in the limit of purely uniform distribution [4].

In a recent paper, Pradhan, Hansen, and Hemmer [7] showed that for a bundle which is close to the complete break down (i.e., imminent failure), a crossover in ξ from a value 5/2 to 3/2 is observed when the threshold distribution approaches the critical distribution. Critical distribution in their case is the distribution in which the lowest threshold of the remaining intact fibers is equal to one-half that of the strongest. This crossover has also been observed with other load sharing rules [8]. We are however interested in looking at the distribution of total avalanche size and a crossover from a power-law behavior with $\xi=5/2$ to a non-mean-field, nonuniversal behavior for smaller Δ is observed near a critical distribution. This interesting behavior is due to the presence of class A fibers. In the present model, the critical distribution corresponds to $\sigma_2=0.5$. We emphasize that in Ref. [7], the proximity of x_0 (the threshold of the weakest intact fiber) to the the critical threshold (=0.5) leads to the crossover behavior whereas in the present case it is the proximity of σ_2 to the critical value (0.5) which is at the root of the observed crossover behavior. In a sense, σ_2 is playing a role analogous to x_0 in our model.

The paper is organized as follows: We have already introduced the model above. The critical stress and exponents are obtained in Sec. II A with a special emphasis on the avalanche size distribution in Sec. II B. The concluding remarks are presented in Sec. III.

II. RESULTS AND DISCUSSIONS

A. Critical stress and exponents

To study the dynamics of failure of fibers, we use the recursive dynamics approach [4]. If a fraction f of the total fibers belong to Class A and the remaining $1-f$ to class B, then the uniformity of the distribution demands

$$f=\frac{1}{1-(\sigma_2-\sigma_1)}\int_0^{\sigma_1} d\sigma,$$

so that

$$\sigma_1=\frac{f}{1-f}(1-\sigma_2). \tag{2}$$

The above equation provides a relationship between f, σ_1, and σ_2 and at the same time puts a restriction on the allowed values of the parameter σ_1 as shown below. Any value of $\sigma_1>f$ leads to a value of σ_2 smaller than σ_1 which is not an acceptable distribution [see Eq. (1)].

We now define U_t as the fraction of unbroken fibers after a time step t. Then the redistributed stress at the instant t is $\sigma_t=F/N_t=\sigma/U_t$ where the applied force $F=N\sigma$ and $N_t=NU_t$. The recurrence relations between U_t, U_{t+1} and between σ_t, σ_{t+1} for the GLS are obtained as [4]

$$U_{t+1}=1-P(\sigma_t)=1-P\left(\frac{\sigma}{U_t}\right)$$

and

$$\sigma_{t+1}=\frac{\sigma}{U_{t+1}}=\frac{\sigma}{[1-P(\sigma_t)]} \tag{3}$$

where $P(\sigma_t)$ is the fraction of broken fibers with the redistributed stress σ_t, and is given as

$$P(\sigma_t)=\int_0^{\sigma_t}\rho(\sigma_{\text{th}})d\sigma_{\text{th}}.$$

This dynamics propagates until no further breaking takes place. It should be emphasized that the initial load is so small that the redistributed stress is always less than σ_2 and therefore fibers from class B cannot fail. Thus to initiate the breaking of class B fibers, the redistributed stress at a later time t must exceed σ_2. The fixed point solution for U $(=U^*)$ and $\sigma(=\sigma^*)$ at which no further failure takes place can be obtained using the standard technique of solving the above recursive relations. By substituting $P(\sigma_t)$ in Eq. (3) we get

$$U_{t+1}=1-P\left(\frac{\sigma}{U_t}\right)$$
$$=1-\left[\frac{\sigma_1}{1-(\sigma_2-\sigma_1)}+\frac{1}{1-(\sigma_2-\sigma_1)}\left(\frac{\sigma}{U_t}-\sigma_2\right)\right].$$

At the fixed point,

$$U^*=1-\left[\frac{\sigma_1}{1-(\sigma_2-\sigma_1)}+\frac{1}{1-(\sigma_2-\sigma_1)}\left(\frac{\sigma}{U^*}-\sigma_2\right)\right]$$

giving the following stable fixed point solutions:

$$U^*=\frac{1}{2[1-(\sigma_2-\sigma_1)]}\left(1+\sqrt{1-\frac{\sigma}{\sigma_c}}\right)$$

and

$$\sigma^*=\frac{1}{2}-\frac{1}{2}\sqrt{1-\frac{\sigma}{\sigma_c}} \tag{4}$$

with

$$\sigma_c=\frac{1}{4[1-(\sigma_2-\sigma_1)]}. \tag{5}$$

If the external applied stress is less than σ_c, the system reaches a fixed point. For $\sigma>\sigma_c$, the bundle breaks down completely as both the U^* and σ^* become imaginary. Equation (4) suggests that the redistributed stress σ^* attains the maximum value (=0.5) at σ_c. The critical stress of the mixed model varies with the gap $(\sigma_2-\sigma_1)$ and reduces to the value $\sigma_c=1/4$ for the uniform distribution as $(\sigma_2-\sigma_1)\to 0$. In deriving Eq. (4), σ_t is assumed to be greater than σ_2 while the applied stress when plotted against the redistributed stress shows a discontinuity at σ_1. Beyond σ_1, the external force is increased to break the fiber with threshold strength σ_2, i.e.,

the gap in the threshold distribution is also reflected in the constitutive behavior of the model.

The discontinuity on the other hand imposes some restrictions on the parameters for this calculation to be valid. Since the maximum value of the redistributed stress is equal to 0.5, σ_2 must be less than 0.5 so that some fibers from class B also fail at the critical point. The condition $\sigma_2 < 0.5$, eventually restricts the value of critical stress to be less than 0.5 for any chosen distribution. However, $\sigma_2 = 0.5$ is a limiting case when the redistributed stress at the critical point marginally reaches class B fibers. In short, we must have

$$\sigma_1 < f, \quad \sigma_2 < 0.5.$$

One can define an order parameter O associated with the transition [4] as shown below,

$$O = 2[1 - (\sigma_2 - \sigma_1)]U^* - 1 = (\sigma_c - \sigma)^{1/2} = (\sigma_c - \sigma)^{\beta}.$$

The order parameter goes to 0 as $\sigma \to \sigma_c$ following a power law $(\sigma_c - \sigma)^{1/2}$. Susceptibility can be defined as the increment in the number of broken fibers for an infinitesimal increase of load. Therefore,

$$\chi = \frac{dm}{d\sigma}, \quad \text{where } m = N[1 - U^*(\sigma)].$$

Hence,

$$\chi \propto (\sigma_c - \sigma)^{-1/2} = (\sigma_c - \sigma)^{-\gamma}.$$

The exponents β and γ stick to their mean field values [4,5], i.e., $\beta = \gamma = 1/2$. We conclude that though the discontinuity alters the critical stress, the critical exponents remain unaltered. It is to be noted that the model reduces to the already obtained results in various limits. For example, if class A fibers are absent ($f=0$), $\sigma_c = 1/4(1-\sigma_2)$ and an elastic to plastic deformation is observed [4].

B. Avalanche size distribution

Let us now focus on the avalanche size distribution exponent ξ. Below is shown some of the allowed distributions which satisfy the above-mentioned restrictions.

Case	f	σ_1	σ_2	σ_c
1	0.10	0.08	0.28	0.31
2	0.20	0.19	0.24	0.26
3	0.20	0.15	0.40	0.33
4	0.30	0.25	0.42	0.30
5	0.30	0.29	0.33	0.26
6	0.40	0.35	0.47	0.29

We study the avalanche size distribution numerically by using the method of breaking of the weakest fiber [6]. In the simulation, the fibers are arranged in an increasing order of their threshold strengths. An external force sufficient to break the weakest fiber is applied and the load due to the breaking of this fiber gets redistributed among the remaining intact fibers following the GLS scheme. The number of failed fibers for a fixed external load is recorded until the dynamics reaches a fixed point. Thereafter, the external load is increased further and the above process is repeated until the critical stress is reached.

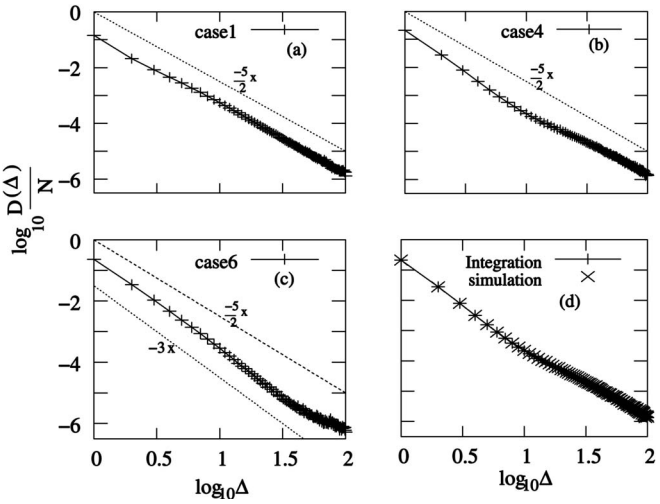

FIG. 2. (a) corresponds to case1 of the table where no crossover is observed. (b) shows a crossover from a nonuniversal behavior to the universal behavior with $\xi = 5/2$ as Δ is increased (case 4). (c) shows an increase in region with nonuniversal behavior (case 6). A line with slope $-5/2$ is drawn in each figure for comparison. In (c) a line with slope -3 is also shown to indicate the apparent power-law behavior. (d) compares the simulation and numerical integration data for case 4 which match identically with each other.

The following interesting observations (Fig. 2) are clearly highlighted. (i) For the cases 1, 2, and 5 of the table, the avalanche size exponent is 5/2. (ii) For the cases 3,4, and 6, there is an apparent power-law behavior for smaller Δ with the exponent which is found to depend on the system parameters. In the examples chosen here the exponent happens to be close to 3. For larger Δ, however, we retrieve the universal mean field behavior with $\xi = 5/2$. Also, (iii) an increase in the region with $\xi \approx 3$ is seen as $\sigma_2 \to 0.5$. These observations establish the following: (i) there is a nonuniversal behavior of $D(\Delta)$ in the small Δ limit, (ii) there is a crossover to the universal behavior in large Δ limit, and (iii) the crossover behavior is prominent as $\sigma_2 \to 0.5$.

The above-mentioned results can be explained by extending the analytical result for the avalanche size distribution obtained by Hemmer and Hansen [6] to the mixed model. The general expression for the avalanche size distribution with GLS is given as

$$\frac{D(\Delta)}{N} = \frac{\Delta^{\Delta-1}}{\Delta!}\int_0^{x_c} dx\rho(x)\left(1 - \frac{x\rho(x)}{Q(x)}\right)\left(\frac{x\rho(x)}{Q(x)}\right)^{\Delta-1} \times \exp\left(-\Delta\frac{x\rho(x)}{Q(x)}\right), \tag{6}$$

where x is the redistributed stress and $Q(x)$ is the fraction of unbroken fibers at x. The upper limit of the integration (x_c) is the redistributed stress at the critical point. The right-hand side of Eq. (6) is broken into two parts, $D_1(\Delta)$ and $D_2(\Delta)$ for

the mixed model with any allowed values of σ_1 and σ_2 [where $\rho(x)=\rho=1/(1-\sigma_2+\sigma_1)$].

As long as the redistributed stress is restricted to the class A fibers,

$$Q(x) = \frac{1-\sigma_2+\sigma_1-x}{1-\sigma_2+\sigma_1},$$

we have

$$D_1(\Delta) = \frac{\Delta^{\Delta-1}}{\Delta!}\frac{1}{1-\sigma_2+\sigma_1}\int_0^{\sigma_1} dx\left(\frac{1-\sigma_2+\sigma_1-2x}{x}\right) \times\left[\frac{x}{1-\sigma_2+\sigma_1-x}\exp\left(-\frac{x}{1-\sigma_2+\sigma_1-x}\right)\right]^{\Delta}. \tag{7}$$

When the redistributed stress belongs to the second block (class B), we have

$$Q(x) = \frac{1-x}{1-\sigma_2+\sigma_1}$$

and

$$D_2(\Delta) = \frac{\Delta^{\Delta-1}}{\Delta!}\frac{1}{1-\sigma_2+\sigma_1}\int_{\sigma_2}^{0.5} dx\left(\frac{1-2x}{x}\right) \times\left[\frac{x}{1-x}\exp\left(-\frac{x}{1-x}\right)\right]^{\Delta}. \tag{8}$$

A close inspection shows that Eq. (8) corresponds to a situation where class A fibers are absent and the results match exactly with Pradhan *et al.* [7] where a crossover in the avalanche size exponent from 5/2 to a value 3/2 is observed as $\sigma_2 \to 0.5$. Here, the presence of class A fibers necessitates the simultaneous study of Eqs. (7) and (8) for the total avalanche size distribution. For distributions which are closer to the critical distribution, Eq. (8) yields exponent $\xi=3/2$ for smaller Δ, but the contribution from Eq. (7) modifies this small Δ behavior.

The results obtained by numerically integrating Eqs. (7) and (8) match identically with the numerical simulation results [Fig. 2(d)]. We observe a sharp fall of $D_1(\Delta)$ [Eq. (7)] which points to the fact that the avalanches of smaller sizes are contributed mainly by the breaking of class A fibers (Fig. 3). The point of intersection of the two integrals yields Δ_c which is the value of the avalanche size where the crossover takes place. The variation of Δ_c for three different cases are shown in Fig. 3. Incidentally in the examples presented here, Δ_c increases with σ_2. If we look at a particular critical distribution (Fig. 4), a crossover from an apparent power-law behavior of $D(\Delta)$ with exponent ξ close to 3 for small Δ to a universal behavior with $\xi=3/2$ is observed.

We now discuss the numerical integration and simulation results in the light of Eqs. (7) and (8). With a change of variable $x \to x/(1-\sigma_2+\sigma_1-x)$, we can rewrite Eq. (7) in the following form:

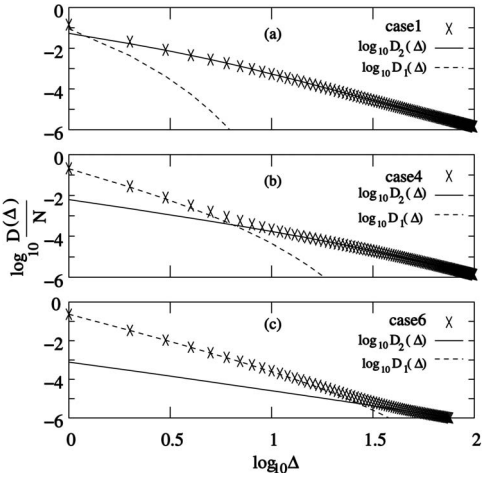

FIG. 3. (a), (b), and (c) present the numerical integration results showing an increase in Δ_c (defined in the text) as $\sigma_2 \to 0.5$. The symbol corresponds to $\log_{10}D(\Delta)/N=\log_{10}(D_1(\Delta)+D_2(\Delta))$ whereas $\log_{10}D_1(\Delta)$ and $\log_{10}D_2(\Delta)$ are drawn to compare their relative magnitudes.

$$D_1(\Delta) = \frac{\Delta^{\Delta-1}}{\Delta!}\int_0^{x_m}\frac{1-x}{x(1+x)^2}e^{(\ln x-x)\Delta}dx, \tag{9}$$

where $x_m=\sigma_1/(1-\sigma_2)$. The argument of the exponential term has a maximum at $x=1$ which is outside the range of integration and hence the saddle point integration method cannot be applied [9]. Expanding the term $1/(1+x)^2$ in a power series and then using the incomplete gamma function [10], we arrive at the following result (see the Appendix):

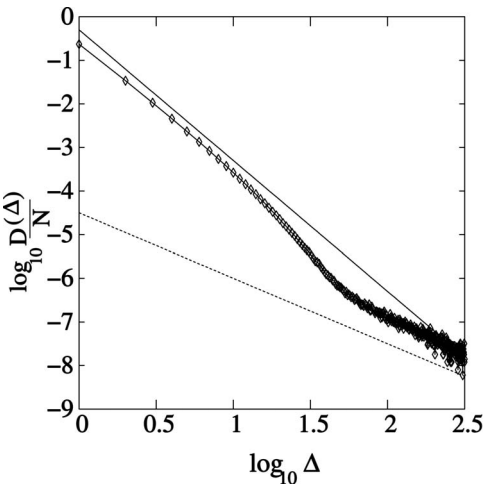

FIG. 4. Avalanche size distribution for a particular critical threshold distribution with $f=0.4$. Thick line corresponds to a slope of −3 and dotted line to −3/2. The asymptotic behavior clearly is $D(\Delta) \sim \Delta^{-3/2}$.

$$D_1(\Delta) = \frac{e^{(1-x_m)\Delta}}{\Delta^{3/2}} x_m^{\Delta} \sum_{q=0}^{\infty} (-1)^q (q+1) x_m^q \times \left(\sum_{k=0}^{\infty} \frac{(x_m\Delta)^k}{(\Delta+q)(\Delta+q+1)\cdots(\Delta+q+k)} - \sum_{k=0}^{\infty} \frac{x_m (x_m\Delta)^k}{(\Delta+q+1)(\Delta+q+2)\cdots(\Delta+q+1+k)} \right). \tag{10}$$

The leading behavior of the infinite series (10) is $\Delta^{-5/2} e^{(1-x_m)\Delta} x_m^{\Delta}$ which justifies the nonuniversality observed in numerical simulations in the small Δ limit. The question therefore remains why does the nonuniversal behavior become prominent as $\sigma_2 \to 0.5$. The behavior of $D_2(\Delta)$ [Eq. (8)] for smaller $\Delta (\ll \Delta_c)$ is at the root of this. When $\sigma_2 \to 0.5$, $D_2(\Delta)$ goes as $\Delta^{-3/2}$ and hence the contribution from $D_1(\Delta)$ wins over to produce a prominent nonuniversal behavior. The small Δ behavior of $D(\Delta)$ is therefore non-mean-field and nonuniversal when $\sigma_2 \to 0.5$. On the other hand, if $\sigma_2 \ll 0.5$, x_m is relatively smaller and the contribution from class A fibers decays very fast as Δ increases and one observes a mean-field universal behavior almost for the entire range of Δ. We also observe a non-power-law behavior for small Δ when σ_1 is very small and σ_2 is close to criticality as is expected from the analytical result. However for a given σ_2 (~ 0.5), larger x_m leads to a nonuniversal behavior up to larger Δ. The crossover value Δ_c is thus roughly given by the value of Δ for which $D_2(\Delta)$ crosses over from a $\Delta^{-3/2}$ behavior to $\Delta^{-5/2}$ behavior.

III. CONCLUSIONS

In conclusion, we have studied a mixed fiber bundle with a discontinuous but uniform threshold distribution and GLS. Discontinuity leads to a functional dependence of the critical stress on the system parameters σ_1, σ_2, and f and also imposes restrictions on the allowed values of these parameters. Although the critical exponents are unchanged, there is a nontrivial change in the burst avalanche distribution behavior where discontinuity leads to a nonuniversal, non-mean-field behavior for small Δ. We would like to emphasize that nonuniversality becomes prominent only when $\sigma_2 \to 0.5$. For large Δ limit, the behavior is however universal and mean field. If $f=0$ or $\sigma_2 \ll 0.5$, the nonuniversal behavior completely disappears. The nonuniversality in $D(\Delta)$ is also seen for other distributions [9]. The beauty of our model is that the nonuniversal behavior is tunable with the system parameters and there is a crossover from nonuniversality to universality in the limit of large Δ. One should also note that the imminent failure of the bundle (i.e., final stages of the breakdown process) is the same as in Ref. [7] because the effect of class A fibers essentially vanishes in that limit.

ACKNOWLEDGMENTS

The authors thank S. Banerjee, P. Bhattacharyya, B. K. Chakrabarti, Y. Moreno, S. Pradhan, and S. K. Rai for useful help and suggestions.

APPENDIX

In this appendix, we shall indicate how to arrive at Eq. (10) of the text starting from Eq. (9). Equation (9) can be written as

$$D_1(\Delta) = \frac{e^{\Delta}}{\Delta^{3/2}} \int_0^{x_m} \frac{1-x}{(1+x)^2} x^{\Delta-1} e^{-\Delta x} dx.$$

Let

$$f(\Delta) = \int_0^{x_m} \frac{1-x}{(1+x)^2} x^{\Delta-1} e^{-\Delta x} dx = \int_0^{x_m} (1-x) x^{\Delta-1} e^{-\Delta x} \left(\sum_{q=0}^{\infty} (-1)^q (q+1) x^q \right) dx = \sum_{q=0}^{\infty} (-1)^q (q+1) \int_0^{x_m} (1-x) x^{\Delta+q-1} e^{-\Delta x} dx.$$

The integral can be further written as

$$\int_0^{x_m} x^{\Delta+q-1} e^{-\Delta x} dx - \int_0^{x_m} x^{\Delta+q} e^{-\Delta x} dx = \frac{1}{\Delta^{\Delta+q}} \int_0^{x_m\Delta} y^{\Delta+q-1} e^{-y} dy - \frac{1}{\Delta^{\Delta+q+1}} \int_0^{x_m\Delta} y^{\Delta+q} e^{-y} dy.$$

Using the power series expansion of incomplete gamma function [10]

$$= \frac{1}{\Delta^{\Delta+q}} \left(e^{-x_m\Delta} \sum_{k=0}^{\infty} \frac{(x_m\Delta)^{\Delta+q+k}}{(\Delta+q)(\Delta+q+1)\cdots(\Delta+q+k)} \right) - \frac{1}{\Delta^{\Delta+q+1}} \times \left(e^{-x_m\Delta} \sum_{k=0}^{\infty} \frac{(x_m\Delta)^{\Delta+q+1+k}}{(\Delta+q+1)(\Delta+q+2)\cdots(\Delta+q+1+k)} \right).$$

Rearranging terms, we get

$$f(\Delta) = e^{-x_m\Delta} x_m^{\Delta} \sum_{q=0}^{\infty} (-1)^q (q+1) x_m^q \times \left(\sum_{k=0}^{\infty} \frac{(x_m\Delta)^k}{(\Delta+q)(\Delta+q+1)\cdots(\Delta+q+k)} - \sum_{k=0}^{\infty} \frac{x_m (x_m\Delta)^k}{(\Delta+q+1)(\Delta+q+2)\cdots(\Delta+q+1+k)} \right),$$

i.e., Eq. (10).

[1] B. K. Chakrabarti and L. G. Benguigui, *Statistical Physics of fracture and Breakdown in Disordered Systems*, (Oxford University Press, Oxford, 1997); M. Sahimi, *Heterogeneous Materials II: Nonlinear Breakdown Properties and Atomistic Modelling* (Springer-Verlag Heidelberg, 2003); H. J. Herrmann and S. Roux, *Statistical Models of Disordered Media* (North-Holland, Amsterdam, 1990).

[2] F. T. Peirce, J. Text. Inst. **17**, 355 (1926); H. E. Daniels, Proc. R. Soc. London, Ser. A **183**, 404 (1945); B. D. Coleman, J. Appl. Phys. **29**, 968 (1958); R. L. Smith, Proc. R. Soc. London, Ser. A **372**, 539 (1980); R. da Silveria, Am. J. Phys. **67**, 1177 (1999); S. Zapperi, P. Ray, H. E. Stanley, and A. Vespignani, Phys. Rev. Lett. **78**, 1408 (1997); J. V. Andersen, D. Sornette, and K. T. Leung, *ibid.* **78**, 2140 (1997).

[3] S. Pradhan and B. K. Chakrabarti, Int. J. Mod. Phys. B **17**, 5565 (2003); P. C. Hemmer, A. Hansen, and S. Pradhan, e-print cond-mat/0602371, in *Modelling Critical and Catastropic Phenomena in Geoscience*, edited by P. Bhattacharyya and B. K. Chakrabarti (Springer, Berlin, 2006). p. 27.

[4] S. Pradhan, P. Bhattacharyya, and B. K. Chakrabarti, Phys. Rev. E **66**, 016116 (2002); P. Bhattacharyya, S. Pradhan, and B. K. Chakrabarti, *ibid.* **67**, 046122 (2003).

[5] Y. Moreno, J. B. Gomez, and A. F. Pacheco, Phys. Rev. Lett. **85**, 2865 (2000).

[6] P. C. Hemmer and Alex Hansen, J. Appl. Mech. **59**, 909 (1992); A. Hansen and P. C. Hemmer, Trends Stat. Phys. **1**, 213 (1994); A. Hansen and P. C. Hemmer, Phys. Lett. A **184**, 394 (1994).

[7] S. Pradhan, A. Hansen, and P. C. Hemmer, Phys. Rev. Lett. **95**, 125501 (2005); S. Pradhan, A. Hansen, and P. C. Hemmer, Phys. Rev. E **74**, 016122 (2006). S. Pradhan and A. Hansen, Phys. Rev. E **72**, 026111 (2005).

[8] F. Raischel, F. Kun, and H. J. Herrmann, Phys. Rev. E **74**, 035104 (2006).

[9] M. Kloster, A. Hansen, and P. C. Hemmer, Phys. Rev. E **56**, 2615 (1997).

[10] M. Abramowitz and I. A. Stegun, *Handbook of Mathematical functions with Formulas, Graphs and Mathematical Tables* (Courier Dover, New York, 1965).